Journal of Alloys and Compounds 559 (2013) 69–75

Contents lists available at SciVerse ScienceDirect

Journal of Alloys and Compounds

journal homepage: www.elsevier.com/locate/jalcom

Pulse reverse electrodeposition of Pt–Co alloys onto carbon cloth electrodes

Napapat Chaisubanan [a], Nisit Tantavichet [a,b,*]

[a] Department of Chemical Technology, Faculty of Science, Chulalongkorn University, Bangkok 10330, Thailand
[b] Center of Excellence on Petrochemical and Materials Technology, Chulalongkorn University, Bangkok 10330, Thailand

ARTICLE INFO

Article history:
Received 13 November 2012
Received in revised form 16 January 2013
Accepted 18 January 2013
Available online 29 January 2013

Keywords:
Pt–Co alloy
Pulse reverse electrodeposition
Electrocatalyst
Dissolution
Proton exchange membrane fuel cell

ABSTRACT

Galvanostatic pulse reverse (PR) electrodeposition of Pt–Co alloys onto pretreated carbon cloth from sulfate solutions has been conducted. The aim is to utilize the anodic current applied during the reverse time to manipulate the morphology and composition of the Pt–Co alloys through a dealloying process. The cathodic current density was found to have a strong effect on the amount and the morphology of the deposited Pt–Co, but not on its composition, over the tested range (20–200 mA cm^{-2}). A higher current density enhances the Pt–Co nucleation process leading to smaller and finer grained Pt–Co alloy electrodeposits, and ultimately to a higher electroactive surface area. Applying the anodic current over a current density range of 50–200 mA cm^{-2} does not substantially alter the amount, morphology or composition of the deposited Pt–Co alloys, with the Pt contents remaining between 91 and 94 mol%. For the PR electrodeposition under the conditions studied, regardless of the magnitude applied, the anodic current does not indicate any dissolution of the Pt–Co alloy deposits, which is supported by the anodic dissolution experiment. Thus, the morphology and composition of the Pt–Co alloy deposits produced by PR electrodeposition are not significantly different from those produced by pulse current electrodeposition at the same cathodic current density.

1. Introduction

There has been a fairly recent vast increase in the application of metal or metal alloy coatings by electrodeposition in diverse areas, such as decoration, corrosion protection [1], ultra large scale integrated circuit fabrication [2], sensors [3–5] and electrode fabrications to use in electrochemical reactions [6,7]. In addition, electrodeposition can also be used to prepare Pt electrocatalyst layers for use in proton exchange membrane fuel cells (PEMFCs) [8–17]. In conventional methods, Pt has to be synthesized and loaded on the carbon (C) supports first (Pt/C). The Pt/C is then mixed with ionomers to form a colloidal solution and subsequently painted or sprayed onto the carbon paper or carbon cloth electrode to form the Pt catalyst electrode. On the other hand, the fabrication of Pt catalyst electrodes by electrodeposition is a single step process where the synthesis of Pt particles and their application onto the electrode take place simultaneously. In addition, the typical methods for Pt-based alloy catalyst electrode fabrication for use in PEMFCs may require a high temperature heat-treatment for the alloying process, which adds more steps and can lead to the formation of larger Pt-alloy particles [18–24]. Electrodeposition, in contrast, can fabricate the Pt-alloy catalyst electrodes in a single step without the need for high temperature heat-treatment [25–30].

For the galvanostatic electrodeposition, different current waveforms, including direct current (DC) electrodeposition, pulse current (PC) or pulse reverse current (PR) electrodeposition, can be applied. Pulse electrodeposition (PC and PR) is widely accepted to be superior to DC electrodeposition since the metal coatings prepared by PC electrodeposition consist of smaller and finer grained structures [8,10,12,29,31–37], which lead to a higher surface area [10]. In addition, unlike DC electrodeposition which has the applied current density as the only controlling parameter, PC electrodeposition has various operating parameters, namely the cathodic current density (i_C), on-time (T_{on}), off-time (T_{off}), duty cycle (ratio of on-time to the pulse cycle period) and frequency, to control the electrodeposition process, to produce deposits with desired properties. PR electrodeposition has the capability to improve the deposit uniformity over that achieved by DC or PC plating by preferentially dissolving overplated areas during the reverse-time (T_{rev}) where an anodic current density (i_A) is applied. For metal alloy deposition of some systems, such as Ni–Fe and Co–Fe, the use of PR electrodeposition can also affect the deposit composition differently than that of PC electrodeposition [38–40]. The benefit of PR electrodeposition of noble metals, such as Pt, may be minimal since they may be stable and may not dissolve during the reverse-time. However, the bi-metal electrodeposition of Pt and a

* Corresponding author at: Department of Chemical Technology, Faculty of Science, Chulalongkorn University, Bangkok 10330, Thailand. Tel.: +66 2 218 7677; fax: +66 2 255 5831.
E-mail address: Nisit.T@chula.ac.th (N. Tantavichet).

0925-8388/$ - see front matter © 2013 Elsevier B.V. All rights reserved.
http://dx.doi.org/10.1016/j.jallcom.2013.01.079

non-noble metal, such as Co, may benefit from the use of PR electrodeposition to manipulate the physical and chemical properties of the Pt-non noble metal alloy through the electrochemical dealloying process of the less noble metal. The preferential dissolution of the non-noble metal from the Pt alloy structure can lead to a more porous and higher Pt content deposit, which can improve its catalytic performance.

In this present work, we investigate the PR electrodeposition of Pt–Co alloys onto pretreated carbon cloths in sulfate solutions. Pt–Co alloys are widely considered as possible candidates for cathode electrocatalysts in PEMFCs due to their higher electrocatalytic activity towards the oxygen reduction reaction (ORR) compared to pure Pt or other Pt-based alloys [19,20,41–48]. The morphological and structural characteristics and compositions of the Pt–Co electrodeposited catalyst layers were studied by scanning electron microscopy (SEM), energy-dispersive spectroscopy (EDX), and X-ray diffractometry (XRD). The main focus of the research reported here is on the effect of the reverse current applied during the reverse-time where the dealloying of Co from the electrodeposited Pt–Co alloys is expected to take place, since this can result in the altered morphology and composition of the Pt–Co alloy deposits from those prepared by PC electrodeposition.

2. Experimental

2.1. Preparation of pretreated carbon cloth

The pretreated carbon cloth was prepared by applying two sub-layers, one hydrophobic and one hydrophilic, based on previously reported work [17]. The hydrophobic layer was prepared from a mixture of a carbon black (Vulcan XC-72), PTFE (60 wt.%) (Aldrich) and isopropanol (Fluka) with a PTFE to carbon black weight ratio of 30:70 and was applied onto a 5 cm^2-carbon cloth (Electrochem, Inc.) until having the loading of 1.9 mg cm^{-2}. Then, a hydrophilic layer consisting of a Nafion 117 ionomer (Fluka) and glycerol (Fluka) with a Nafion to glycerol weight ratio of 50:50 was painted on top to have the total hydrophilic loading of 0.8 mg cm^{-2}. Finally, the prepared non-catalyst electrode was dried at 300 °C for 2 h.

2.2. Electrodeposition of Pt–Co on the pretreated carbon cloth

Electrodeposition of the Pt–Co alloys was conducted in a two compartment electrochemical cell, separated by a Nafion 115 membrane, using a standard three-electrode system. The pretreated carbon cloth was placed in a compartment containing a solution of 0.01 M $H_2PtCl_6{\cdot}6H_2O$ (Fluka), 0.1 M $CoSO_4{\cdot}7H_2O$ (Fluka) and 0.5 M H_2SO_4. The titanium gauze used as the counter electrode was placed in the other compartment containing 0.5 M H_2SO_4. The Ag/AgCl reference electrode (3 M KCl, Metrohm) was placed in the same compartment as the working electrode to reduce the voltage drop when monitoring the electrode potential during the electrolysis. During the electrodeposition the solution was stirred by a magnetic stirrer at 300 rpm. All electrodeposition experiments were carried out using an Autolab PGSTAT 10 Potentiostat (Eco Chemie) equipped with voltage multiplier to widen the monitored potential range. The electrode responses recorded during the electrodeposition are reported in the Ag/AgCl scale.

The cathodic and anodic current densities were evaluated over the range of 20–200 mA cm^{-2} and 50–200 mA cm^{-2}, respectively. Each cathodic pulse was set to have 10 mC cm^{-2} of charge density. Unless otherwise stated, all electrodeposition experiments were carried out until a total net charge density of 2 C cm^{-2} was passed where the total cathodic and anodic charge densities for the PR electrodeposition were fixed at 4 and 2 C cm^{-2}, respectively. After the electrodeposition, the Pt–Co electrodeposited carbon cloth was removed from the solution and dried at 80 °C for 2 h. The total amount of the Pt–Co alloy catalyst electrodeposited on the electrode was estimated from the weight difference between that before and after the electrodeposition.

2.3. Analysis of the Pt–Co deposit

The morphology and composition of the electrodeposited Pt–Co catalyst layers were studied by SEM (JEOL: JSM 6400) equipped with EDX. The structural characteristics of the electrodeposited catalyst layers were examined by XRD (Bruker AXS: D8 Discover).

The electrochemical active surface area (EAS) of each Pt–Co alloy deposit was studied based on underpotential of hydrogen desorption using the electrochemical technique. The carbon cloth coated with the Pt–Co electrodeposited catalyst layer was placed in a single compartment electrochemical cell containing nitrogen purged 0.5 M H_2SO_4 solution with a Pt gauze counter electrode and a Ag/AgCl reference electrode. The cyclic voltammetry (CV) was scanned between −0.4 and −1.4 V (Ag/AgCl) at a scan rate of 20 mV s^{-1} using an Autolab PGSTAT 10 Potentiostat. The EAS (in m^2 gPt^{-1}) was estimated from the coulometric charge of the hydrogen desorption peak using the following equation [49–52]:

$$\mathrm{EAS} = 0.1\frac{q_{\mathrm{H}}}{W_{\mathrm{Pt}} \times q_{\mathrm{H,ref}}} \quad (1)$$

where q_H is the total charge density (mC cm^{-2}) associated with the hydrogen underpotential desorption (calculated by integrating the hydrogen desorption peak of the CV curve with the subtraction of the baseline due to the double layer capacity), W_{Pt} is the Pt loading (mg cm^{-2}) and $q_{H,ref}$ is the charge density (0.21 mC cm^{-2}), corresponding to the adsorption of a monolayer of hydrogen on a polycrystalline Pt surface.

3. Results and discussion

The XRD results of the Pt–Co deposits prepared from the PR electrodeposition at a cathodic current density of 20 mA cm^{-2} and different anodic current densities, along with that of the Pt electrodeposit prepared by DC electrodeposition at 10 mA cm^{-2}, are shown in Fig. 1. The inset shows the lattice parameter and Pt–Pt mean atomic distance of the Pt and Pt–Co electrodeposits, as estimated from the XRD patterns. The XRD patterns of the Pt–Co deposits prepared from PR electrodeposition using other cathodic current densities are similar to those shown in Fig. 1 and so are not shown here. The XRD patterns of the Pt–Co deposits prepared by PR electrodeposition show noticeable shifts of the Pt(111), Pt(200), Pt(220), Pt(311) and Pt(222) peaks to higher 2θ values compared to those in the Pt electrodeposited catalyst. No additional peaks appear on the XRD patterns of the Pt–Co deposits from that of the Pt deposit. The lattice parameter and Pt–Pt mean atomic distance of the Pt–Co electrodeposited catalysts become smaller than that of the Pt electrodeposited catalyst. These results indicate the contraction of Pt lattices due to the incorporation of smaller Co atoms into the face cubic center (fcc) structure of the larger Pt structure [19,42,53,54] during Pt–Co electrodeposition. Also, there is no evidence of metallic Co (the reflection of Co(111) is expected to appear at a $2\theta = 44.8$) or Co oxides found from the XRD patterns, which implies that the Co atoms are incorporated into the Pt structure in the form of an alloy.

The SEM images of the Pt–Co deposits prepared from different electrodeposition conditions are shown in Fig. 2. For comparison purposes, the Pt–Co electrodeposits prepared by DC (current density and charge density of 10 mA cm^{-2} and 2 C cm^{-2}, respectively) and PC (cathodic current density of 20 mA cm^{-2} and charge density of 2 and 4 C cm^{-2}) electrodeposition were also conducted and their SEM images are shown in Fig. 3. The amount and composition of the Pt–Co deposits prepared under different conditions are showed in Table 1. SEM images (Fig. 2) indicate that the catalyst layers prepared by PR electrodeposition at the lowest cathodic current density (20 mA cm^{-2}) consist of large Pt–Co particles. The size of the Pt–Co particles is reduced at higher cathodic current densities. In addition, compared to the deposit produced by the DC electrodeposition at 10 mA cm^{-2} (Fig. 3a), the deposits obtained from the pulse electrodeposition under the conditions studied (Figs. 2 and 3b and c) have smaller grains and finer structures due to the ability to apply a significantly larger current density during the pulse electrodeposition without violation of mass transfer limitations [55]. A higher applied current density generally leads to more energy being available to enhance the nucleation process during electrocrystalization and so produce smaller-grained particles [56]. However, when comparing the morphologies of the Pt–Co alloy deposits obtained under different anodic current densities, the SEM results reveal no significant difference in the Pt–Co deposited structure, even though anodic current densities as low as 20 mA cm^{-2} and as high as 200 mA cm^{-2} were used. In fact, the

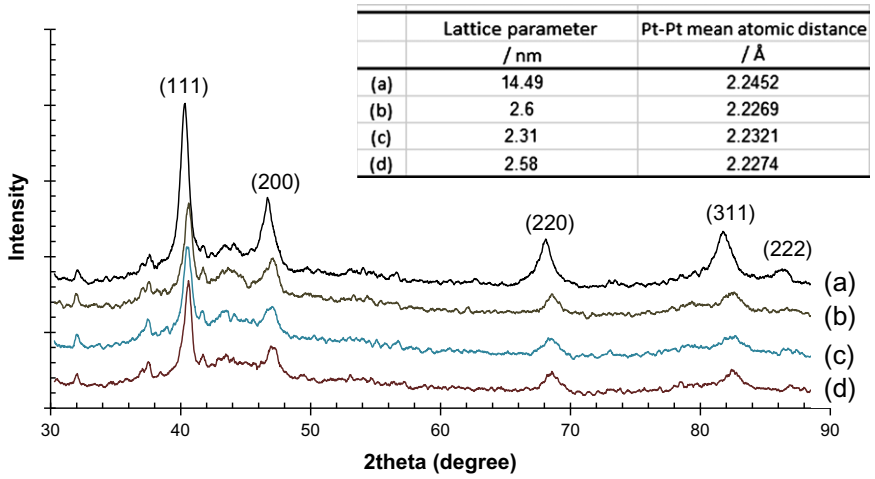

Fig. 1. X-ray diffraction patterns of the (a) Pt deposit prepared by DC electrodeposition at 10 mA cm^{-2} and (b–d) Pt–Co alloy deposits prepared by PR electrodeposition at a cathodic current density of 20 mA cm^{-2} and anodic current densities of (b) 50, (c) 100 and (d) 200 mA cm^{-2}. The inset presents the lattice parameter and the Pt–Pt mean atomic distance of the Pt and Pt–Co deposits prepared under the above conditions.

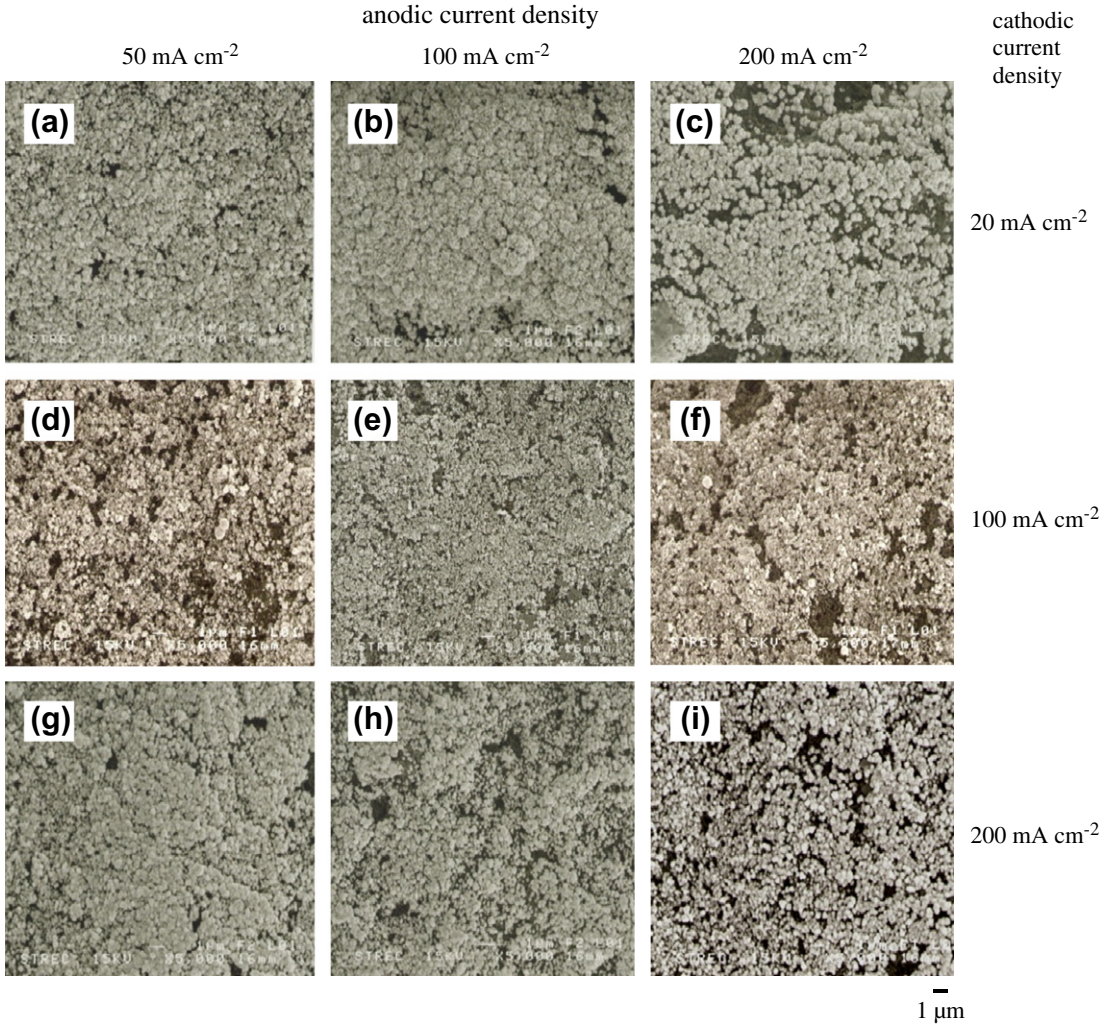

Fig. 2. SEM images (×5000) of the Pt–Co alloy deposits prepared by PR electrodeposition at different cathodic current densities of (a–c) 20, (d–f) 100 and (g–i) 200 mA cm^{-2} and anodic current densities of (a, d, and g) 50, (b, e, and h) 100 and (c, f, and i) 200 A cm^{-2} for cathodic and anodic charge densities of 4 and 2 C cm^{-2}, respectively.

morphologies of the Pt–Co deposits prepared by the PR electrodeposition (Fig. 2a–c) and PC electrodeposition (Fig. 3b), where no anodic current was applied, are relatively similar. These results imply that the magnitude of the applied anodic current or the pulse mode may not have any profound effect on the deposit morphology of the Pt–Co deposits.

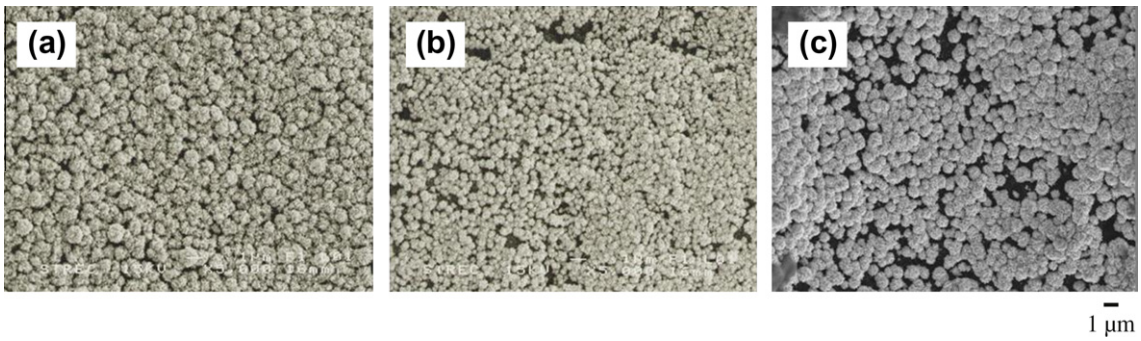

Fig. 3. SEM images (×5000) of the Pt–Co alloy deposits prepared by (a) DC electrodeposition at 10 mA cm^{-2} and 2 C cm^{-2} and (b and c) PC electrodeposition at a cathodic current density of 20 mA cm^{-2} and charge densities of (b) 2 and (c) 4 C cm^{-2}.

Table 1
Deposit loading, chemical composition, current efficiency and electrochemical surface area of the as-deposited Pt–Co alloys prepared under different electrodeposition conditions.

Mode	i_C (mA cm^{-2})	T_{on} (s)	i_A (mA cm^{-2})	T_{rev} (s)	q_{on} (C cm^{-2})	q_{rev} (C cm^{-2})	Deposit loading (mg cm^{-2})	Pt:Co (mol%)	Current efficiency[a] (%)	EAS (m^2 gPt)
DC	10	200	–	–	2	–	0.3768	92:8	37.9	54
PC	20	0.5	–	0.03	2	–	0.1739	93:7	17.5	–
			–	0.03	4	–	0.4493	93:7	22.6	69
PR	20	0.5	50	0.1	4	2	0.4493	93:7	22.6	72
			100	0.05	4	2	0.4278	93:7	21.5	72
			200	0.025	4	2	0.4928	92:8	24.8	71
	100	0.2	50	0.1	4	2	0.2464	91:9	12.4	221
			100	0.05	4	2	0.2029	93:7	10.2	271
			200	0.025	4	2	0.2029	93:7	10.2	200
	200	0.1	50	0.1	4	2	0.0579	91:9	2.9	821
			100	0.05	4	2	0.0539	94:6	2.7	799
			200	0.025	4	2	0.0579	94:6	2.9	820

[a] Current efficiency is calculated based on the applied cathodic charge density.

Like the morphology, the amount of Pt–Co deposited on the electrode was found to be strongly affected by the magnitude of the cathodic current density applied (Table 1). The amount of Pt–Co deposited on the carbon cloth tends to decrease as the cathodic current density is raised, falling from about 0.45 mg at 20 mA cm^{-2} down to 0.20 and 0.054 mg at 100 and 200 mA cm^{-2}, respectively. The decrease in the amount of Pt–Co catalyst deposited by an increase in the cathodic pulse amplitude is likely to be due to an increase in the hydrogen evolution reaction (HER). Thermodynamically, Pt preferentially deposits much easier than Co since the standard reduction potentials of $PtCl_6^{2-}$ and Co^{2+} ions to metallic metals are approximately at 0.76 and −0.28 V (SHE), respectively. However, the reduction potentials of these two metals are separated by the hydrogen evolution reaction. That means at high applied current densities, like ones used in this study, the electrodeposition of Pt–Co alloy is normally accompanied by the HER. During electrodeposition at the high applied current density, the surface concentration of Pt ions reaches low level and approaches the mass transfer limitation, while surface concentration of Co ions remains relatively high, so that the Co reduction and the HER can proceed at the higher rates. Although the HER is thermodynamically easier to proceed compared to the Co deposition reaction, under the appropriate conditions (i.e., at high negative potentials and in a plating bath with a limited amount of H^+ ions) the Co deposition can proceed at a faster rate than the HER [57]. However, at the very high negative cathodic potentials and in the high acidic plating bath (Fig. 4), the HER is the predominant cathodic reaction so that the amount and the current efficiency of Pt–Co deposits are decreased by an increase in the cathodic pulse amplitude (Table 1). The other factor that also facilitates the HER for the Pt–Co deposition at the higher cathodic current densities is the higher active area for the HER of the Pt–Co catalysts produced at the higher cathodic pulse amplitudes, since Pt is a good catalyst for the HER and the small-grained catalysts (Fig. 2) lead to the higher active area for the HER (this will be discussed in detail later).

Unlike the magnitude of the cathodic current density, the magnitude of the anodic current density (i_A) does not seem to affect the amount of Pt–Co deposited on the electrodes. Interestingly, the amounts of Pt–Co alloys electrodeposited by PR electrodeposition are similar to those produced by PC electrodeposition using the same cathodic charge density of 4 C cm^{-2} (i.e., about 0.44 mg cm^{-2} for an i_C of 20 mA cm^{-2}). The amount and morphology of the Pt–Co deposited by different anodic current density amplitudes indicate that the pulse plating mode and the magnitude of the anodic current density do not substantially affect the physical properties of the Pt–Co alloy deposits.

The composition of the Pt–Co alloys prepared by PR electrodeposition is not significantly affected by the magnitude of the cathodic and anodic current densities, since the Pt content remains between 91% and 94% for all electrodeposition conditions evaluated (Table 1). As discussed earlier, the Pt–Co alloy electrodeposition at the high cathodic current densities takes place under the mass transfer limitation of Pt and the excess current is used for the Co deposition and the HER. If the amount of H^+ ions in the plating baht is limited, the HER is diffusion limited and Co deposition makes up the deficit so that the Pt–Co alloy with the higher Co content is expected [57–59]. On the other hand, for the Pt–Co electrodeposition in the high acidic plating baht, the HER proceeds at the faster rate than the Co deposition reaction. Thus, the excess part of the cathodic current is used for the HER and the composition of the Pt–Co alloys is unaffected by the cathodic pulse amplitude. Interestingly, the Pt content of the Pt–Co alloy obtained from PC

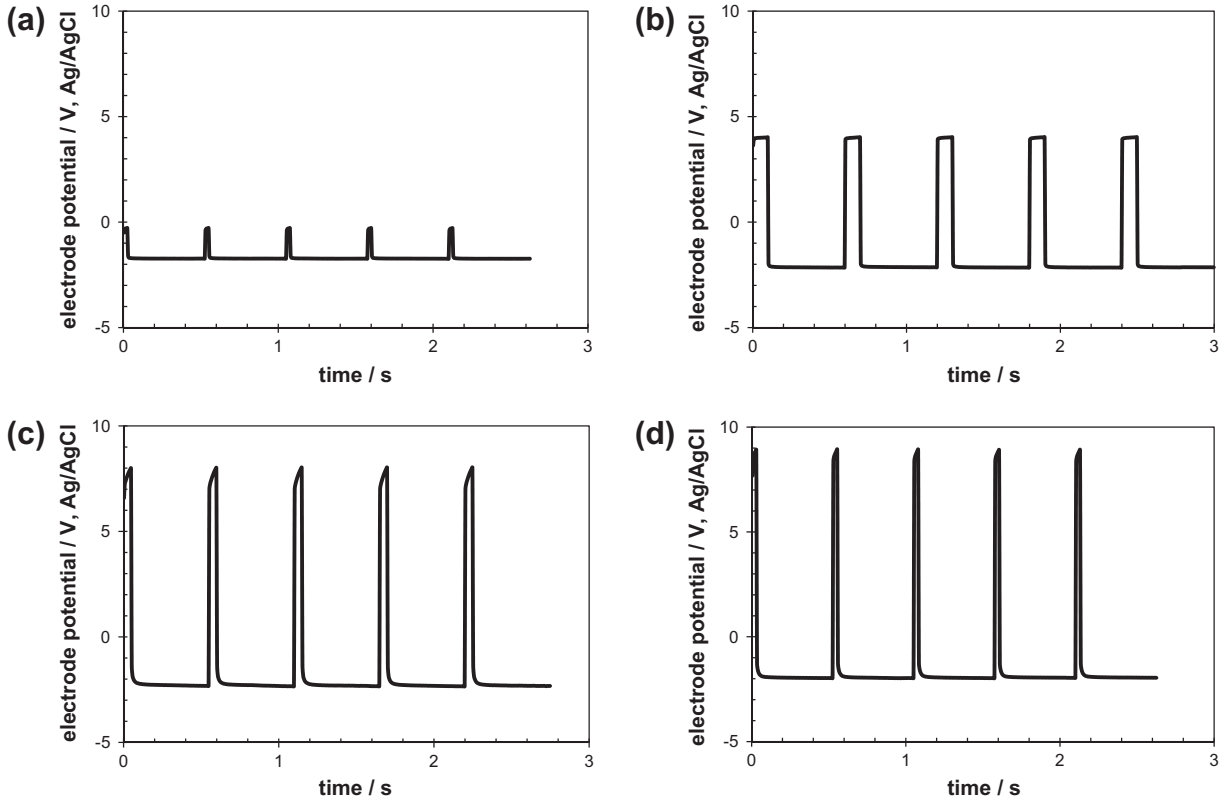

Fig. 4. Electrode response during (a) PC electrodeposition at a cathodic current density of 20 mA cm^{-2} and (b–d) PR electrodeposition at a cathodic current density of 20 mA cm^{-2} and anodic current densities of (b) 50, (c) 100 and (d) 200 mA cm^{-2}.

electrodeposition (93%) also falls in the range of those obtained by PR electrodeposition. It has been reported previously that the applied current density for DC and PC electrodeposition has only a small effect on the composition of the Pt–Co alloys [29]. It has been reported that decreasing the Pt content in the Pt–Co deposit could be achieved more easily by reducing the amount of Pt present in the electrolyte [26,29,60,61]. However, little research has focused on the application of PR electrodeposition for Pt–Co electrodeposition.

The electrode responses during PR and PC electrodeposition were recorded (shown in Fig. 4 for PR and PC electrodeposition at a cathodic current density of 20 mA cm^{-2}). The open circuit potential of the Pt–Co deposited carbon cloth in the plating solution was found to be around 1.1 V. During the reverse-time, the anodic potentials rise to 4, 8 and 9 V for anodic current densities of 50, 100 and 200 mA cm^{-2}, respectively, which are much higher than the open circuit potential or the electrode potential during the off-time of the PC electrodeposition (Fig. 4a). Based on a pourbaix diagram of Pt, Pt is expected to be stable due to the formation of the passive film at high positive potentials. Accordingly, one would expect a significant dissolution of Co from the Pt–Co alloys deposited by the PR electrodeposition, and so should yield an alloy containing a higher Pt content than 93 mol%. However, the Pt content in the Pt–Co alloys produced by PR electrodeposition remains essentially unchanged regardless of the magnitude of the anodic current density applied and again is similar to that produced by PC electrodeposition, as seen in the composition analysis together with the morphological analysis and the amount of Pt–Co alloys deposited. Thus, an applied anodic current density as high as 200 mA cm^{-2} for the total anodic charge density of 2 C cm^{-2} may not dissolve any significant amount of Co from the Pt–Co alloy structure and the only reaction taking place on the Pt–Co deposit surface during the reverse-time is an oxygen evolution reaction ($H_2O \rightarrow \frac{1}{2}O_2 + 2H^+ + 2e^-$).

To test this hypothesis, PR electrodeposition was used to produce Pt–Co alloy coatings on three pretreated carbon clothes at a fixed cathodic current density of 20 mA cm^{-2} under the same three anodic current densities as performed previously. Then, the Pt–Co alloy coated carbon clothes were dried (80 °C for 2 h), weighed and analyzed by SEM and EDX. Each Pt–Co alloy coated carbon cloth was then placed in the working electrode compartment of the two compartment electrochemical cell containing the same solution in each compartment as used for the electrodeposition. The dissolution tests were done by applying anodic pulse waveforms with anodic current densities of 200 mA cm^{-2} for 0.025 s, 100 mA cm^{-2} for 0.05 s and 50 mA cm^{-2} for 0.1 s, (same waveforms used for the electrodeposition, but without the cathodic pulse) on the Pt–Co coated carbon clothes produced by the PR electrodeposition. After the total anodic charge density of 2 C cm^{-2} was passed, the Pt–Co coated carbon cloths were removed, dried, weighed and subjected to morphological and chemical analysis to monitor any dissolution of the Pt–Co deposits or changes in the morphology or Pt–Co alloy composition after the anodic pulsing, similar to when the PR electrodeposition was carried out. The electrode responses during the anodic pulse tests (data not shown) are similar to those for the anodic electrode responses during the PR electrodeposition (Fig. 4b–f).

The % weight change and composition analysis results (Table 2) and corresponding SEM images (Fig. 5) indicate no (or very little) dissolution of the Pt–Co alloy deposits during the anodic pulse since there is less than a 2% weight change, the compositions remain at ~93 mol% Pt and the morphologies show no visible signs of dissolution or morphological change (Fig. 5 vs. Fig. 2a–c) of the Pt–Co deposits before and after the anodic pulse was applied.

Table 2
Weight change and chemical composition of Pt–Co alloys before and after the dissolution tests.

PR electrodeposition	Dissolution pulse current density	wt. Change (%)	Pt:Co before dissolution test	Pt:Co after dissolution test
i_C = 20 mA cm^{-2}; i_A = 50 mA cm^{-2}	50 mA cm^{-2}	−0.24	93:7	93:7
i_C = 20 mA cm^{-2}; i_A = 100 mA cm^{-2}	100 mA cm^{-2}	−1.8	93:7	93:7
i_C = 20 mA cm^{-2}; i_A = 200 mA cm^{-2}	200 mA cm^{-2}	−1.7	92:8	92:8

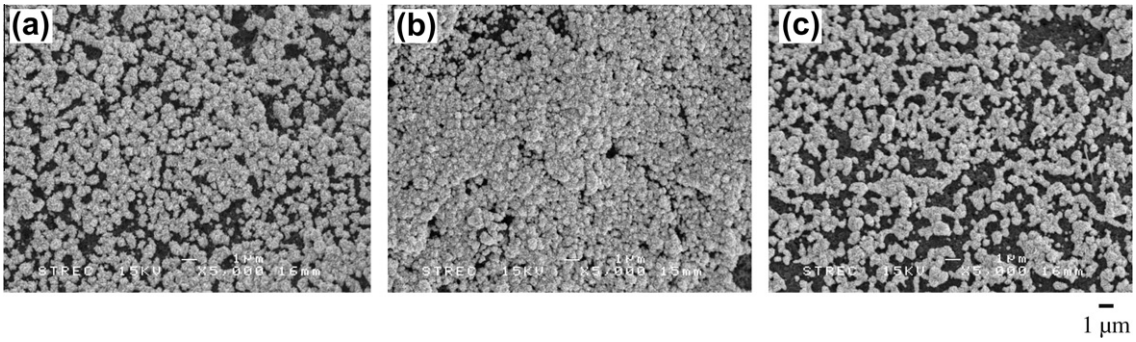

Fig. 5. SEM images (×5000) of the Pt–Co alloy deposits prepared by PR electrodeposition at a cathodic current density of 20 mA cm^{-2} and anodic current densities of (a) 50, (b) 100 and (c) 200 mA cm^{-2}, after the dissolution tests.

Thus, applying an anodic current in the form of PR electrodeposition may not be of benefit in manipulating the morphology and composition of the Pt–Co deposited alloys compared to the conventional PC electrodeposition, since no significant dissolution of the Co from the Pt–Co alloys occurred during the anodic pulse.

In contrast, several studies have previously reported the use of dealloying process to change the morphology and composition of Pt–Co alloys even when no (or a small magnitude of) anodic potential was applied [48,52,62,63]. It was reported that the level of Pt present in the Pt–Co alloy is an important factor in the dissolution process [63]. For very Pt-rich (>90% Pt) Pt–Co alloys, based on the Co dissolution model presented by Hoshi and Co-workers [63], all Co atoms in the second layer are partially covered with Pt atoms or most of the Co atoms present in the Pt–Co alloy structure may form strong bonds directly to Pt (i.e., Co–Pt bonding). It is, then, more difficult to separate Co atoms from the Pt hosted structure. For Pt–Co alloys with a lower Pt content, a number of Co atoms in the second layer are exposed completely without the coverage of Pt atoms present in the first layer [63] or some Co atoms may form Co–Co bonding that is easier to dissolve out of the Pt–Co alloy structure than the Co–Pt bonded atoms [62]. As a result, it is easier for Co atoms to dissolve out of the Pt–Co alloy structure. Thus, it may be possible that the use of the PR electrodeposition can, in fact, manipulate the morphology and composition of the deposited Pt–Co alloys by dissolving parts of the Pt–Co alloys when applying the anodic pulse, but the Pt content in the Pt–Co alloys has to be low enough. As shown above, although the deposition mode and the magnitude of the cathodic current density used in this study have a substantial effect on the deposit morphology, they do not have any profound effect on the composition of the deposited Pt–Co alloy. To decrease the amount of Pt deposited in the Pt–Co alloys, the composition of the plating solution would have to be adjusted in a way to enhance the deposited amount of Co in the Pt–Co alloys. Currently, we are investigating the possibility to utilize the dissolution process in PR electrodeposition to control the structure and composition of the Pt–Co alloys in different plating bath compositions.

Fig. 6 shows the CVs of some Pt–Co coated carbon clothes obtained from DC and pulse (PC and PR) electrodeposition in a N_2-purged 0.5 M H_2SO_4 solution. The calculated EAS values are listed in Table 1. The Pt–Co deposits produced by pulse

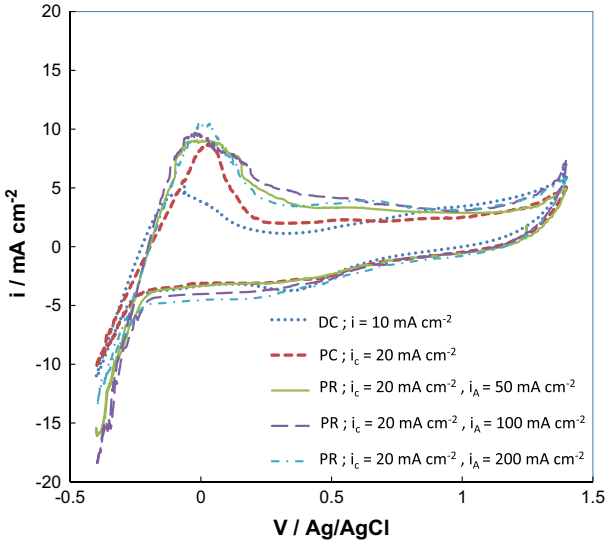

Fig. 6. Cyclic voltammograms (CVs) of Pt–Co deposits prepared by DC electrodeposition at 10 mA cm^{-2}, PC electrodeposition at a cathodic current density of 20 mA cm^{-2} and PR electrodeposition at a cathodic current density of 20 mA cm^{-2} and anodic current densities of 50, 100 and 200 mA cm^{-2}, in N_2-purged 0.5 M H_2SO_4.

electrodeposition have a significantly higher EAS than that produced by DC electrodeposition. In addition, the Pt–Co deposits prepared under the same cathodic current density have relatively similar EAS regardless of the magnitude of the applied anodic current density, whilst increasing the cathodic current density leads to a higher EAS. These results support previous findings that the cathodic current density has a profound effect, whereas the anodic current density shows no effect, on the morphology of the Pt–Co deposits, and those with finer and smaller grained structures yield a higher EAS.

4. Conclusion

The electrodeposition of Pt–Co alloys onto pretreated carbon cloths by PR electrodeposition reveals that the anodic current pulse

does not significantly dissolve the deposited Co part from the Pt–Co alloys and so cannot manipulate the physical and chemical properties of the deposited Pt–Co alloys through dealloying of the less noble Co metal. Overall, the Pt–Co alloys prepared by PC or PR electrodeposition have smaller and finer grained structures with higher EAS than that prepared by DC electrodeposition. The Pt contents were found to be between 91 and 94 mol% for all electrodeposition conditions studied, regardless of the deposition mode and the magnitudes of the cathodic and anodic current densities applied. The cathodic current density shows a significant effect on the amount, morphology and ultimately EAS of the deposited Pt–Co alloys. The applied anodic current, on the other hand, shows no substantial effect on the amount and morphology of the Pt–Co alloys even though a wide range of the anodic current densities (200–50 mA cm^{-2}) is applied. The physical and chemical properties of the Pt–Co alloys produced by the PR electrodeposition do not differ from that produced by the PC electrodeposition. A separate dissolution experiment has shown that the morphology, weight and composition of Pt–Co alloys remain unchanged when only an anodic pulse is applied on the Pt–Co alloy coated carbon cloths. The results of this study indicate that most of the Co atoms in high Pt content Pt–Co alloys are relatively inert towards anodic dissolution when alloyed to Pt so that no or only a very small amount of Co dissolves during the PR electrodeposition. Accordingly, manipulating the morphology and composition of the Pt–Co alloy deposits cannot be achieved by PR electrodeposition.

Acknowledgments

The authors gratefully express their gratitude to the Higher Education Research Promotion and National Research University Project of Thailand, Office of the Higher Education Commission (EN276B), and to the Graduate School of Chulalongkorn University, for financial support during the course of this study.

References

[1] W. Schwarzacher, Electrochem. Soc. Interface 15 (1) (2006) 32–35.
[2] P.C. Andricacos, Electrochem. Soc. Interface 8 (1) (1999) 32–37.
[3] F. Favier, E.C. Walter, M.P. Zach, T. Benter, R.M. Penner, Science 293 (2001) 2227–2231.
[4] E.C. Walter, R.M. Penner, H. Liu, K.H. Ng, M.P. Zach, F. Favier, Surf. Interface Anal. 34 (2002) 409–412.
[5] T. Selvaraju, R. Ramaraj, J. Electroanal. Chem. 585 (2005) 290–300.
[6] M.P. Marceta Kaninski, V.M. Nikolic, G.S. Tasic, Z. Lj, Int. J. Hydrogen Energy 34 (2009) 703–709.
[7] C. Lupi, A. Dell'Era, M. Pasquali, Int. J. Hydrogen Energy 34 (2009) 2101–2106.
[8] K.H. Choi, H.S. Kim, T.H. Lee, J. Power Sources 75 (1998) 230–235.
[9] S.D. Thompson, L.R. Jordan, M. Forsyth, Electrochim. Acta 46 (2001) 1657–1663.
[10] H. Kim, N.P. Subramanian, B.N. Popov, J. Power Sources 138 (2004) 14–24.
[11] N. Rajalakshmi, K.S. Dhathathreyan, Int. J. Hydrogen Energy 33 (2008) 5672–5677.
[12] N. Saibuathong, Y. Saejeng, K. Pruksathorn, M. Hunsom, N. Tantavichet, J. Appl. Electrochem. 40 (2010) 903–910.
[13] J. Li, F. Ye, L. Chen, T. Wang, J. Li, X. Wang, J. Power Sources 186 (2009) 320–327.
[14] A.J. Martín, A.M. Chaparro, B. Gallardo, M.A. Folgado, L. Daza, J. Power Sources 192 (2009) 14–20.
[15] H. Zhang, W. Zhou, Y. Du, P. Yang, C. Wang, Electrochem. Commun. 12 (2010) 882–885.
[16] F. Alcaide, G. Álvarez, J.A. Blázquez, P.L. Cabot, O. Miguel, Int. J. Hydrogen Energy 35 (2010) 5521–5527.
[17] S. Lertviriyapaisan, N. Tantavichet, Int. J. Hydrogen Energy 35 (2010) 10464–10471.
[18] M.-K. Min, J. Cho, K. Cho, H. Kim, Electrochim. Acta 45 (2000) 4211–4217.
[19] M. Neergat, A.K. Shukla, K.S. Gandhi, J. Appl. Electrochem. 31 (2001) 373–378.
[20] A.K. Shukla, M. Neergat, Parthasarathi Bera, V. Jayaram, M.S. Hegde, J. Electroanal. Chem. 504 (2001) 111–119.
[21] P. Yu, M. Pemberton, P. Plasse, J. Power Sources 144 (2005) 11–20.
[22] J.R.C. Salgado, E. Antolini, E.R. Gonzalez, J. Power Sources 141 (2005) 13–18.
[23] N. Martz, C. Roth, H. Fueß, J. Appl. Electrochem. 35 (2005) 85–90.
[24] Y. Lu, R.G. Reddy, Electrochim. Acta 52 (2007) 2562–2569.
[25] A. Lima, C. Coutanceau, J.-M. Léger, C. Lamy, J. Appl. Electrochem. 31 (2001) 379–386.
[26] C. Coutanceau, A.F. Rakotondrainibé, A. Lima, E. Garnier, S. Pronier, J.-M. Léger, C. Lamy, J. Appl. Electrochem. 34 (2004) 61–66.
[27] R.S. Jayashree, J.S. Spendelow, J. Yeom, C. Rastogi, M.A. Shannon, P.J.A. Kenis, Electrochim. Acta 50 (2005) 4674–4682.
[28] A.J. Martín, A.M. Chaparro, L. Daza, J. Power Sources 169 (2007) 65–70.
[29] Y. Saejeng, N. Tantavichet, J. Appl. Electrochem 39 (2009) 123–134.
[30] Y. Ra, J. Lee, I. Kim, S. Bong, H. Kim, J. Power Sources 187 (2009) 363–370.
[31] R.T.C. Choo, J.M. Toguri, A.M. El-Sherik, U. Erb, J. Appl. Electrochem. 25 (1995) 384–403.
[32] G. Holmbom, B.E. Jacobson, J. Electrochem. Soc. 135 (1988) 2720–2725.
[33] W. Kim, R. Weil, Surf. Coat. Tech. 38 (1989) 289–298.
[34] K.P. Wong, K.C. Chan, T.M. Yue, Surf. Coat. Tech. 115 (1999) 132–139.
[35] P.T. Tang, Electrochim. Acta 47 (2001) 61–66.
[36] C.-C. Hu, C.-M. Wu, Surf. Coat. Tech. 176 (2003) 75–83.
[37] A. Ibañez, E. Fatás, Surf. Coat. Tech. 191 (2005) 7–16.
[38] J. Horkans, J. Electrochem. Soc. 128 (1981) 45–49.
[39] P.C. Andricacos, C. Arana, J. Tabib, J. Dukovic, L.T. Romankiw, J. Electrochem. Soc. 136 (1989) 1336–1340.
[40] Y. Liu, M. Pritzker, J. Appl. Electrochem. 33 (2003) 1143–1153.
[41] S. Mukerjee, S. Srinivasan, M.P. Soriaga, J. Mcbreen, J. Electrochem. Soc. 142 (1995) 1409–1422.
[42] N. Travitsky, T. Ripenbein, D. Golodnitsky, Y. Rosenberg, L. Burshtein, E. Peled, J. Power Sources 161 (2006) 782–789.
[43] L. Xiong, A.M. Kannan, A. Manthiram, Electrochem. Commun. 4 (2002) 898–903.
[44] J.R.C. Salgado, E. Antolini, E.R. Gonzalez, J. Phys. Chem. B 108 (2004) 17767–17774.
[45] E. Antolini, J.R.C. Salgado, M.J. Giz, E.R. Gonzalez, Int. J. Hydrogen Energy 30 (2005) 1213–1220.
[46] H.A. Gasteiger, S.S. Kocha, B. Sompalli, F.T. Wagner, Appl. Catal. B – Environ. 56 (2005) 9–35.
[47] K. Jayasayee, V.-A.T. Dam, T. Verhoeven, S. Celebi, F.A. de Bruijn, J. Phys. Chem. C 113 (2009) 20371–20380.
[48] S. Axnanda, K.D. Cummins, T. He, D.W. Goodman, M.P. Soriaga, Chem. Phys. Chem. 11 (2010) 1468–1475.
[49] E. Antolin, L. Giorgi, A. Pozio, E. Passalacqua, J. Power Sources 77 (1999) 136–142.
[50] A. Pozio, M. De Francesco, A. Cemmi, F. Cardellini, L. Giorgi, J. Power Sources 105 (2002) 13–19.
[51] M. Alvisi, G. Galtieri, L. Giorgi, R. Giorgi, E. Serra, M.A. Signore, Surf. Coat. Tech. 200 (2005) 1325–1329.
[52] L. Liu, E. Pippel, R. Scholz, U. Gösele, Nano Lett. 9 (2009) 4352–4358.
[53] X. Zhang, K.-Y. Chan, J. Mater. Chem. 100 (2002) 1203–1206.
[54] T. Lopes, E. Antolini, F. Colmati, E.R. Gonzalez, J. Power Sources 164 (2007) 111–114.
[55] D. Landolt, Mass transport in pulse plating, in: J.C. Puippe, F.H. Leaman (Eds.), Theory and Practice of Pulse Plating, AESF, Orando, FL, 1986, pp. 55–72.
[56] J.C. Puippe, Influence of pulse plating on crystallization, in: J.C. Puippe, F.H. Leaman (Eds.), Theory and Practice of Pulse Plating, AESF, Orlando, FL, 1986, pp. 17–40.
[57] O.E. Kongstein, G.M. Haarberg, J. Thonstad, J. Appl. Electrochem. 37 (2007) 669–674.
[58] K. Leistner, A. Krause, S. Fähler, H. Schlörb, L. Schultz, Electrochim. Acta 52 (2006) 170–176.
[59] K. Leistner, S. Oswald, J. Thomas, S. Fähler, H. Schlörb, L. Schultz, Electrochim. Acta 52 (2006) 194–199.
[60] M. Cortés, S. Matencio, E. Gómez, E. Vallés, J. Electroanal. Chem. 627 (2009) 69–75.
[61] S. Woo, I. Kim, J.K. Lee, S. Bong, J. Lee, H. Kim, Electrochim. Acta 56 (2011) 3036–3041.
[62] F.-J. Lai, W.-N. Su, L.S. Sarma, D.-G. Liu, C.-A. Hsieh, J.-F. Lee, B.-J. Hwang, Chem. Eur. J. 16 (2010) 4602–4611.
[63] Y. Hoshi, R. Ozawa, E. Tada, A. Nishikata, T. Tsuru, Corros. Sci. 65 (2012) 512–519.